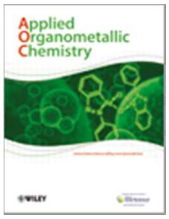

Stable *trans* isomer as the kinetic and theromodynamic product for the oxidative addition of MeI to cycloplatinated(II) complexes comprising isocyanide ligands

Journal:	*Applied Organometallic Chemistry*
Manuscript ID	AOC-17-0793
Wiley - Manuscript type:	Full Paper
Date Submitted by the Author:	13-Oct-2017
Complete List of Authors:	Shahsavari, Hamid R.; Institute for Advanced Studies in Basic Sciences (IASBS), Chemistry Babadi Aghakhanpour, Reza; Department of Chemistry, Institute for Advanced Studies in Basic Sciences (IASBS), Zanjan, 45137-66731, Iran, Hossein-Abadi, Mojdeh ; Institute for Advanced Studies in Basic Sciences kia, Reza ; Sharif University of Technology Raithby, Prof. Paul R. ; University of Bath, Department of Chemistry
Keywords:	Isocyanide ligands, Cycloplatinated complexes, Oxidative addition, Kinetic, Mechanism, DFT calculations

Note: The following files were submitted by the author for peer review, but cannot be converted to PDF. You must view these files (e.g. movies) online.

Scheme 1.cdx
Scheme 2.cdx
Scheme 3.cdx

Stable *trans* isomer as the kinetic and theromodynamic product for the oxidative addition of MeI to cycloplatinated(II) complexes comprising isocyanide ligands

Hamid R. Shahsavari,[a] Reza Babadi Aghakhanpour,[a] Mojdeh Hossein-Abadi,[a] Reza Kia,[b]* and Paul R. Raithby[c]*

[a]Department of Chemistry, Institute for Advanced Studies in Basic Sciences (IASBS), Yousef Sobouti Blvd., Zanjan 45137-66731, Iran

[b]Chemistry Department, Sharif University of Technology, P.O. Box 11155-3516, Tehran, Iran

[c]Department of Chemistry, University of Bath, Claverton Down, BA2 7AY, Bath, UK

Email: shahsavari@iasbs.ac.ir (H.R.S.); rkia@sharif.edu (R.K.).

Keywords: Isocyanide ligands • Cycloplatinated complexes • Oxidative addition • Kinetic • Mechanism • DFT calculations.

Abstract

The present investigation introduces a new series of cycloplatinated(II) complexes, with the general formula Pt(O-bpy)(Me)(CN-R)] (R = benzyl, 2-naphtyl and *tert*-butyl), which are able to generate the stable *trans*-Pt(IV) product in the solution after the reaction with iodomethane. In fact, the *trans* product is both the kinetic and thermodynamic product of the reaction; this observation was supported by DFT calculations. These Pt(II) complexes are supported by 2,2'-bipyridine *N*-oxide (O-bpy) and one of several isocyanides as the cyclometalated and ancillary ligands, respectively. These new Pt(II) complexes undergo oxidative addition with MeI to give the corresponding *trans*-Pt(IV) complexes. All the complexes were identified employing the multi-nuclear NMR spectroscopy and single crystal X-ray crystallography. The kinetic investigations were also performed for the oxidative addition reactions in order to measure the reaction rates; the reaction was followed by UV-Vis spectroscopy. The rates obtained follow the trend CN-^{t}Bu > CN-Bz > CN-2Np for the CN-R

ligands in the Pt(II) complexes. The order can be related to the degree of electron-donation of the R group (*tert*-butyl > benzyl > 2-naphtyl).

Introduction

It is well-known that the kinetics and mechanism of oxidative addition of alkyl halides to unsaturated platinum(II) complexes obeys the classical S_N2 mechanism[1-6], except a few exceptions which occur under specific reaction conditions.[6-8] The large negative $\Delta S^{\neq}$ value observed is indisputable evidence for this assertion.[2, 9-11] Interestingly, there are many reports in the literature that theoretical calculations support the experimental kinetic data.[12-18] In the previous investigations, particularly for the reported cycloplatinated(II) complexes, it has been proven that the roles of cyclometalated and ancillary ligands are very important in determining the reaction rate.[19-34] For example, the ancillary monophosphanes, containing a wide range of substituents, are the appropriate choices for tuning the oxidative addition reaction rate of cycloplatinated(II) complexes due to their various electronic and steric effects.[19]

The *trans* addition of RX (alkyl halides) to cyclometalated platinum(II) complexes affords the *trans* isomer as the kinetic product, passing through a cationic intermediate with a halide counter anion. The cationic intermediate can rearrange to a *cis* intermediate in order to create the *cis* isomer as the thermodynamic product. Excluding a few cases,[27, 35] the *trans* isomer cannot be usually isolated and crystallized because it is not stable in the solution and converts to the thermodynamic product (*cis*) before crystallization. The rate of this *trans*-*cis* conversion is determined by the type of cyclometalated or ancillary ligands present. In this regard, we have recently compared four different cycloplatinated (II) complexes, incorporating the same ancillary ligand but different cyclometalated ligands.[35] Therein, it was indicated that the presence of electron-withdrawing atoms on the cyclometalated ligands causes that the rate of *trans*-*cis* isomerization to be decreased substantially. In fact, by using the 2,2'-bipyridine *N*-oxide (O-bpy) as the cyclometalated ligand, the rate became so slow that the *trans* isomer could be isolated and crystallized. However, the *trans* isomer was eventually isomerized to the thermodynamically stable *cis* product after several days in solution. These findings motivated us to design a new cyclometalated system with O-bpy that it able to stabilize the kinetic *trans* product, permanently.

In order to continue our investigations in the field of kinetics and mechanism of oxidative addition reactions at platinum(II) centers,[5, 19, 24, 35-37] we have now designed a series of new Pt(II) complexes, incorporating 2,2'-bipyridine *N*-oxide (cyclometalated ligand) and isocyanides (ancillary ligand) concurrently. Secondly, the oxidative addition of iodomethane (MeI) to these Pt(II) complexes was performed to obtain the corresponding *trans*-Pt(IV) complexes. After characterization of the new complexes by multi-nuclear NMR spectroscopy and X-ray crystallography, the oxidative addition reactions were kinetically investigated using the UV-vis spectroscopy, supported by the theoretical calculations. In this work, by employing the carbon-donor isocyanide ligands instead of common phosphane ligands, the *trans* isomer was quite stable in the solution.

Results and Discussions

Synthesis and Characterization of Complexes

The synthetic route for the new Pt(II) and Pt(IV) complexes is summarized in Scheme 1. Full NMR characterization, including ^{1}H, $^{13}C\{^{1}H\}$, ^{195}Pt, DEPT 135° and two dimensional techniques (COSY, HSQC), was performed for the complexes in order to better identify the new structures. The results are embedded in the Supporting Information Figures S1-S29 while the numerical data are summarized in Experimental Section. The parent complex [Pt(O-bpy)(Me)(SMe_2], **A**,[38] was reacted with 1 equivalent of each isocyanide ligands and gave the pure Pt(II) complexes [Pt(O-bpy)(Me)(CN-R)] (R = benzyl (**1a**), 2-naphtyl (**2a**) and *tert*-butyl (**3a**)). These resulting Pt(II) complexes were treated with excess iodomethane, producing the corresponding *trans*-Pt(IV) complexes [Pt(O-bpy)$(Me)_2$I(CN-R)] (R = benzyl (**1b**), 2-naphtyl (**2b**) and *tert*-butyl (**3b**)).

The ^{1}H NMR spectra for the Pt(II) derivatives all include a distinguishing singlet signal with platinum satellites in the aliphatic region which can be assigned to methyl ligand. For **1a**, in addition to the signal assigned to the Me ligand, a singlet signal is observed for the two benzylic protons of benzyl isocyanide ligand which is flanked with platinum satellites ($^{4}J_{PtH}$ = 11.3 Hz). However, in the case of **3a**, a large and sharp signal appears at δ = 1.61 ppm which represents 9 equivalent protons of *tert*-butyl group. In the aromatic region, for **1a**-**3a**, two distinct doublet resonances with platinum satellites are observed for $H^{3'}$ and H^{6} protons of O-bpy ligand which

indicates that the C^N chelate did not open during the reaction of **A** with isocyanides. Another discrete signal assignable to the H^3 proton of O-bpy appears as a sharp doublet signal. This signal is considerably deshielded to near 10 ppm due to being directly in contact through space with oxygen atom of the O-bpy.[35, 38-40]

Similar to the ^{1}H NMR spectra, in the $^{13}C\{^1H\}$ NMR spectra of Pt(II) complexes, the carbon of methyl ligand in all cases exhibits a singlet with a large coupling constant value to platinum center ($^1J_{PtC}$). The $^{13}C\{^1H\}$ NMR spectrum of **1a** contains a singlet signal at δ = 48.0 ppm with $^3J_{PtC}$ = 10 Hz which is attributed to the benzylic carbon of benzyl isocyanide ligand. This signal grows down-phase in the corresponding DEPT 135° spectrum as the only secondary carbon. Besides, for **3a**, a signal appears at δ = 48.0 ppm as singlet which represents the three equivalent carbons of *tert*-butyl group. As far as is possible, the aromatic carbon atoms are characterized and the results summarized in Experimental Section in detail. However, for all the Pt(II) compounds, the most distinctive signal in the aromatic region corresponds to the $C^{2'}$ of O-bpy ligand which is directly connected to the platinum center, having a large Pt-$C^{2'}$ coupling constant. Since this carbon is located *trans* to isocyanide ligand, the Pt-$C^{2'}$ coupling constant value can be a reliable benchmark for the level of intrinsic *trans* effect assignable to the isocyanide ligands. As can be seen, these coupling values are almost the same, indicating no difference between the *trans* effects of isocyanides despite of the presence of very different R groups in their structures. Finally, it should be noted that the ligating carbon of isocyanide, as another distinct carbon, appear between the aromatic signals as a broad peak due to the coupling with platinum and nitrogen atoms.[41]

In the case of Pt(IV) complexes, the aromatic regions for both the ^{1}H and $^{13}C\{^1H\}$ NMR spectra are similar to those of their Pt(II) derivatives with only smaller coupling constants for the Pt(IV) center in relation to their Pt(II) parents. This observation is due to the increasing in the oxidation state of the platinum center from +2 to +4 during the oxidative addition reaction which can be related to a formal change of hybridation state from dsp^2 to d^2sp^3.[27] All the ^{1}H and $^{13}C\{^1H\}$ NMR spectra for **1b-3b** possess two different singlet signals with platinum satellites in their aliphatic regions which are attributed to the two different methyl ligands; one is *trans* to I and the other one is *trans* to N (see Experimental for the details). In the ^{1}H NMR spectrum of **1b**, the signal for benzylic protons appears at δ = 5.15 ppm with $^4J_{PtH}$ = 8.5 Hz. In its $^{13}C\{^1H\}$ NMR

spectrum, the benzylic carbon appears δ = 48.6 ppm as a singlet; this signal appears down phase in the DEPT 135° spectrum, like its Pt(II) parent. For **3b**, in the ^{1}H NMR spectrum, a singlet resonance is observed at δ = 1.70 ppm for the methyl groups of *tert*-butyl moiety. The carbons of these methyl groups appear as a sharp singlet in the $^{13}C\{^{1}H\}$ NMR spectrum at δ = 30.45 ppm.

In order to better characterization of the structures of the complexes, single crystal X-ray diffraction was performed for the Pt(II) complex **1a** and its corresponding Pt(IV) complex, **1b**. The ORTEP plots of **1a** and **1b** are shown in Figure 1 and the geometrical parameters are embedded in the Tables S1 and S2. The crystal data and refinement parameters of **1a** and **1b** are summarized in Table 1. The crystals for both complexes (**1a** and **1b**), being of suitable quality for the X-ray crystallography, were obtained by slow layer diffusion of *n*-hexane into their solutions in dichloromethane. Interestingly, both complexes crystallize in the same monoclinic crystal system and the same space group of $P2_1/c$. The structure of **1a** confirms that the benzyl isocyanide ligand, as a strong carbon donor, can be located *trans* to the C ligating atom of O-bpy chelate.[42] The phenyl moiety of benzyl isocyanide ligand is almost perpendicular to the molecule plane. As can be seen, in the structure of **1b**, the Me and I ligands are located *trans* to each other. The structure of **1b** confirms that the *trans* isomer can be isolated and crystallized. Due to the larger steric hindrance in the structure of **1b**, the perpendicularity of phenyl moiety decreases and tilts to one side in relation to that of **1a**. The crystal packing of both 1a and 1b is stabilized by the intermolecular C–H···O and π···π interactions. The interesting feature of the crystal packing of 1b is the *zigzag* connection of the neighboring molecules along the b-axis through the intermolecular C–H···O interaction (Figure 2).

<<Scheme 1>>

<< Figure 1>>

<< Figure 2>>

Table 1. Crystal data and refinement parameters for **1a** and **1b**

	1a	**1b**
Empirical formula	$C_{19}H_{17}N_3OPt$	$C_{20}H_{20}IN_3OPt$
Formula mass	498.44	640.38
Crystal system	monoclinic	monoclinic
Space group	$P2_1/n$	$P2_1/n$
θ_{max} (°)	29	30
a (Å)	5.4813(1)	17.9672(5)
b (Å)	14.8066(3)	8.4217(3)
c (Å)	20.3545(4)	13.0861(5)
β (°)	92.874(2)	92.837(4)
V (Å^3)	1649.88(6)	1977.69(12)
Z	4	4
D_{calc} (Mg/m^3)	2.007	2.151
μ (mm^{-1})	8.515	8.669
F(000)	952	1200
Index ranges	$-7 \le h \le 7$	$-25 \le h \le 22$
	$-20 \le k \le 20$	$-11 \le k \le 11$
	$-27 \le l \le 27$	$-13 \le l \le 18$
No. of measured reflections	20369	11214
No. of independent reflections/R_{int}	4321/0.0321	5754 /0.041
No. of observed reflections $I > 2\sigma(I)$	3887	4785
No. of parameters	218	235
Goodness-of-fit (GOF)	1.121	1.06
R_1 (observed data)	0.0203	0.0409
wR_2 (all data)[a]	0.0420	0.0630

Kinetic and Mechanism Study

The oxidative addition reactions of Pt(II) complexes with excess MeI were kinetically investigated in CH_2Cl_2 solvent. Each reaction was monitored using the disappearance of MLCT (Metal to Ligand Charge Transfer) band in the UV-visible spectrum of the corresponding cycloplatinated(II) complex.[19, 24, 37] Figure 3a-c represent the changes in the UV-vis spectra of **1a-3a** at 298 K. Also the k_{obs} values, being the *pseudo*-first-order rate constants, were measured by nonlinear least-squares fitting of the absorbance-time curves to a first-order equation. The graphs of k_{obs} values *versus* the concentration of MeI were drawn for five temperatures which gave straight line plots with no intercept (Figure 3d-f for **1a-3a**, respectively). The slopes of these straight lines afford the overall second-order rate constants (k_2) for the different temperatures. The k_2 values for all the Pt(II) complexes are collected in Table 2. Besides, the activation parameters were calculated from Eyring plots (Figure 4) for the reactions and numerical data are listed in the Table 2.

<< Figure 3>>

<< Figure 4>>

Table 2. Second-order rate constants[a] and activation parameters[b] for the reaction of [Pt(O-bpy)(Me)(CN-R)], **1a-3a**, with MeI in CH_2Cl_2.

Complex	λ_{max} / nm	10^3 k_2 / L mol^{-1} s^{-1} at different temperatures					$\Delta H^{\#}$ / kJ mol^{-1}	$\Delta S^{\#}$ / JK^{-1}mol^{-1}
		10 °C	20 °C	25 °C	30 °C	35 °C		
1a	385	0.79	1.23	1.56	1.98	2.52	37.9 ± 0.1	-169 ± 1
2a	380	0.20	0.46	0.75	1.10	1.53	57.4 ± 0.2	-113 ± 1
3a	378	0.88	1.57	2.14	2.75	3.50	31.0 ± 0.1	-194 ± 1

[a] Estimated errors in k_2 values are ± 2%.

[b] Activation parameters were calculated from the temperature dependence of the second-order rate constant in the usual way using Eyring equation.

Based on the calculations, it was obvious that all the reactions followed the second order kinetics (first order for both cycloplatinated(II) complex and the MeI reagent) suggesting a common S_N2 mechanism for the reactions. The large negative $\Delta S^{\#}$ values (Table 2) provides peremptory evidence for the proposed mechanism. A schematic view of the S_N2 mechanism for

the present reactions is presented in Scheme 2. The nucleophilic attack of the Pt(II) entity (**a**) on the MeI reagent generates the cationic intermediate (**c**) with iodide as its counter anion. This step passes through a transition state (**b**). In the next step, **c** can be converted to the *trans*-Pt(IV) complex (**d**), as the kinetic product, by coordination of iodine to the platinum center. Based on our previous experiences,[19, 24, 35] it was expected that the intermediate **c** undergoes a rearrangement to make the second intermediate **e** and consequently *cis*-Pt(IV) product. However, the NMR spectroscopic results show that this rearrangement did not occur in the solution even after a long time (more than 1 month). Evidently, this is due to the fact that the CN-R ligand cannot be situated *trans* to the methyl group which is necessary for such rearrangement. Actually, both CN-R and Me ligands, as two strong carbon σ-donors, exhibit large *trans* effects which makes the rearrangement so hard and almost impossible to occur. Even, this rearrangement cannot happen in the presence of bulky R groups in the structure of CN-R ligands in order to decrease the steric hindrance. Then, the *trans*-Pt(IV) product (**d**) behaves as both the kinetic and thermodynamic product.

<<Scheme 2>>

As can be concluded from Table 2, at a constant temperature (for example 25 °C), the reaction of **1a** with MeI is occurs almost two times faster than that observed for **2a**. In this regard, the reaction of **3a** is also performed 1.4 and 2.8 time faster than that of **1a** and **2a**, respectively (**3a** (^{t}Bu) > **1a** (Bz) > **2a** (2-Np)). Obviously, the electron-donating capability of the R group (^{t}Bu > Bz > 2-Np) has a key role in determining the rate of the reactions. With increasing the electron-donating capability of the R group, the platinum center becomes more negative and more able to perform the oxidative addition reaction faster.

Since the isocyanides family are very strong σ-donors, the reactions of cycloplatinated(II) complexes containing isocyanide ancillary ligand with MeI are dramatically faster than their similar derivatives with different ancillary ligands (for example phosphanes).[35] When the cyclometalated ligand changes to ppy (deprotonated 2-phenylpyridine), the reaction rate became so fast and is similar to phosphane complexes (ppy is 23 times faster than O-bpy).[35] For this reason, the presence of the oxygen in the cyclometalated fragment (O-bpy), as a strong electron-withdrawing atom, remarkably decreases the rates of the reactions.

DFT Calculations

In order to shed some light on the mechanism of the reaction of Pt(II) complexes with MeI in CH_2Cl_2, DFT (Density Functional Theory) calculations were performed for the typical reaction of **1a** with MeI. In this way, the structures of **1a** and **1b** together with the **TS** (transition state), **IMt** (*trans* intermediate) and **IMc** (*cis* intermediate) were optimized without imposing any symmetry constraints (Figure 5). Additionally, the dichloromethane solvation effects were modelled by Conductor-like Polarizable Continuum Model (CPCM).[30] The calculated energy profile for the oxidative addition reaction is also depicted in Figure 6. In the energy profile, the summation of energies of **1a** and MeI is considered to be zero and the other elements in the profile vary accordingly. As can be seen, **TS** is generated through the nucleophilic attack of $\mathbf{5d_Z^2}$ atomic orbital of Pt(II) center on the **σ*** of Me-I bond. In the structure of **TS**, the methyl group of the MeI is planar and the Pt-C(Me)-I angle is almost linear with a value close to 180°.[30, 35] The dotted lines between Pt and C(Me) and also between C(Me) and I indicate that the Pt-C(Me) bond is gradually being formed whereas the C(Me)-I bond is gradually being broken. In the next step, the unstable **TS** is converted to the **IMt** which in turn has two pathways to choose for conversion (**IMc** or **1b**). As supported by DFT calculations, the **IMt** → **IMc** isomerization is not energetically affordable for the **IMt** (with the energy barrier of 20.5 kJ/mol) and **IMt** prefers to be converted to the kinetic product (**1b**). As mentioned earlier, the reason for this observation is that the CN-Bz and Me ligands both exhibit strong *trans* effects which causes that the energy level of **IMc** becomes higher than that of **IMt**. In such conditions, the *trans* geometry becomes both thermodynamic and kinetic products. However, in our recent investigation in which phosphane ligand has been instead of isocyanide,[35] the energy level of **IMc** is lower than that of **IMt**. Therein, the **IMt** → **IMc** isomerization is performed easy because the phosphane ligand can be conveniently situated *trans* to methyl ligand and therefore the thermodynamic product has *cis* geometry.

<< Figure 5>>

<< Figure 6>>

Conclusion

A series of cycloplatinated(II) complexes with general formula [Pt(O-bpy)(Me)(CN-R)] (R = benzyl, 2-naphtyl and *tert*-butyl), **1a-3a** were synthesized and characterized spectroscopically. The resulting Pt(II) complexes were reacted with excess MeI to give the corresponding *trans*-cycloplatinated(IV) complexes [Pt(O-bpy)(Me)$_2$I(CN-R)], **1b-3b**. The oxidative addition reactions were kinetically studied by following the UV-vis spectra of the Pt(II) complexes. The kinetic data and the large negative values of $\Delta S^{\#}$ suggest a classical S_N2 mechanism. The observed rates show the trend **3a** > **1a** > **2a** for the reactions of cycloplatinated(II) complexes with MeI which has a direct relation with the electron-donating capability of the R groups in the CN-R ligands (^{t}Bu (**3a**) > Bz (**1a**) > 2-Np (**2a**)). With increasing the electron-donating capability of the R group, the oxidative addition reaction proceeds faster due to the platinum center becoming more negative and therefore the reaction occurs more quickly.

In previous, similar investigations,[19, 35] the proposed mechanism included a *trans-cis* isomerization to produce the thermodynamically stable *cis* product from *trans* kinetic product. But, a key point in these reactions is that the mentioned *trans-cis* isomerization is inhibited in the present reactions. This observation arises from the fact that the CN-R and Me groups, as two strong σ-donors with large *trans* effects, cannot be located *trans* to each other. Therefore the *trans*-Pt(IV) product is both the thermodynamic and kinetic product so that it can be isolated and structurally characterized by X-ray crystallography. Finally, the DFT calculations were typically performed for one of the reactions (**1a** + MeI → **1b**) which supported the experimental data. The energy level of *cis* intermediate (**IMc**) is calculated to be much higher than that of *trans* intermediate (**IMt**) and the conversion of **IMt** → **IMc** has a large energy barrier. Under such conditions, **IMt** prefers to be converted to the Pt(IV) complex (**1b**) which is both the kinetic and thermodynamic product.

Experimental

Procedures and materials

The reactions were performed in the common solvents in the laboratory. The microanalyses for all the new compounds were performed using a vario EL CHNS elemental

analyzer. Also, the melting point values were measured by a Buchi 510. Fourier transform infrared spectroscopy on KBr pellets was performed on a FT IR Bruker Vector 22 instrument. Multinuclear (^{1}H, $^{13}C\{H\}$, ^{195}Pt) NMR spectra together with two dimensional NMR spectra (COSY and HSQC) and DEPT 135° technique were recorded on a Bruker Avance DPX 400 MHz spectrometer at 298 K. All chemical shifts are reported in ppm (part per million) relative to their corresponding external standards ($SiMe_4$ for ^{1}H and $^{13}C\{H\}$ and Na_2PtCl_6 for ^{195}Pt) and also all the coupling constants (*J* values) are given in Hz. All solvents were purified and dried according to standard procedures.[43] UV-vis spectra were recorded using a Perkin-Elmer Lambda 25 spectrophotometer. Benzyl isocyanide and *tert*-butyl isocyanide were purchased from Acros while 2-naphthyl isocyanide was purchased from Sigma-Aldrich. The complex [Pt(O-bpy)(Me)(SMe_2)], **A**,[38] was prepared according to the literature. The NMR labeling for all the ligands are shown in Scheme 3 for clarifying the chemical shift assignments.

<<Scheme 3>>

[Pt(O-bpy)(Me)(CN-Bz)], 1a. To a solution of **A** (200 mg, 0.451 mmol) in CH_2Cl_2 (20 mL), 1 equivalent of CN-CH_2Ph (55 μL, 0.451 mmol, benzyl isocyanide) was added. The reaction mixture was stirred for 3 h at room temperature and then the solution was concentered to small volume (~ 3 mL) under reduced pressure and *n*-pentane (10 mL) was added to give **1a** as a yellow, which was filtered and washed with *n*-pentane (3 × 3 mL) and dried. Yield: 178 mg, 79%; m.p. = 184°C. Elem. Anal. Calcd. for $C_{19}H_{17}N_3OPt$ (498.44) C, 45.78; H, 3.44; N, 8.43. Found: C, 45.62; H, 3.49; N, 8.41. IR (KBr, cm^{-1}): 2181 (s, $\upsilon_{C\equiv N}$). NMR data in $CDCl_3$: $\delta(^{1}H)$ = 0.85 [s, 3H, $^{2}J_{PtH}$ = 83.7 Hz, Pt-Me]; 4.71 [s, 2H, $^{4}J_{PtH}$ = 11.3 Hz, CH_2 of benzyl]; 7.56 [dd, 1H, $^{3}J_{H^{3'}H^{4'}}$ = 7.2 Hz, $^{4}J_{H^{3'}H^{5'}}$ = 1.1 Hz, $^{3}J_{PtH^{3'}}$ = 56.1 Hz, $H^{3'}$ of O-bpy]; 7.86 [dd, 1H, $^{3}J_{H^{5'}H^{4'}}$ = 6.4 Hz, $^{4}J_{H^{5'}H^{3'}}$ = 1.1 Hz, $H^{5'}$ of O-bpy]; 8.51 [dd, 1H, $^{3}J_{H^{6}H^{5}}$ = 5.4 Hz, $^{4}J_{H^{6}H^{4}}$ = 1.1 Hz, $^{3}J_{PtH^{6}}$ = 20.2 Hz, H^6 of O-bpy]; 9.72 [d, 1H, $^{3}J_{H^{3}H^{4}}$ = 8.2, H^3 of O-bpy]; $\delta(^{13}C\{H\})$ = -19.3 [s, 1C, $^{1}J_{PtC}$ = 682 Hz, Pt-Me]; 48.0 [s, 1C, $^{3}J_{PtC}$ = 10 Hz, CH_2 of benzyl]; 125.8 [s, 1C, $^{3}J_{PtC^{3}}$ = 13.6 Hz, C^3 of O-bpy]; 126.9 [s, 2C, C^3 of benzyl]; 129.4 [s, 2C, C^2 of benzyl]; 130.4 [s, 1C, $^{2}J_{PtC^{3'}}$ = 65.7 Hz, $C^{3'}$ of O-bpy], 138.4 [s, 1C, $C^{4'}$ of O-bpy]; 146.6 [broad signal, 1C, C of isocyanide]; 151.0 [s, 1C, $^{2}J_{PtC^{6}}$ = 20.5 Hz, C^6 of O-bpy]; 158.9 [s, 1C, $^{1}J_{PtC^{2'}}$ = 940 Hz, $C^{2'}$ of O-bpy]; $\delta(^{195}Pt)$ = -3952.9 [broad s, 1Pt].

[Pt(O-bpy)(Me)(CN-2Np)], 2a. To a solution of **A** (200 mg, 0.451 mmol) in CH_2Cl_2 (20 mL), 1 equivalent of CN-2-naphthyl (69 mg, 0.451 mmol, 2-Naphthyl isocyanide) was added. The reaction mixture was stirred for 3 h at room temperature and then the solution was concentered to small volume (~ 3 mL) under reduced pressure and *n*-pentane (10 mL) was added to give **2a** as a pale brown, which was filtered and washed with *n*-pentane (3 × 3 mL) and dried. Yield: 229 mg, 95%; m.p. = 180°C. Elem. Anal. Calcd. for $C_{22}H_{17}N_3OPt$ (534.47) C, 49.44; H, 3.21; N, 7.86. Found: C, 49.52; H, 3.24; N, 7.98. IR (KBr, cm^{-1}): 2145 (s, $\upsilon_{C\equiv N}$). NMR data in $CDCl_3$: $\delta(^1H)$ = 1.17 [s, 3H, $^2J_{PtH}$ = 83.9 Hz, Pt-Me]; 7.80 [dd, 1H, $^3J_H{}^{3'}{}_H{}^{4'}$ = 7.5 Hz, $^4J_H{}^{3'}{}_H{}^{5'}$ = 0.8 Hz, $^3J_{PtH}{}^{3'}$ = 54.5 Hz, $H^{3'}$ of O-bpy]; 8.09 [dd, 1H, $^3J_H{}^{5'}{}_H{}^{4'}$ = 6.5 Hz, $^4J_H{}^{5'}{}_H{}^{3'}$ = 0.9 Hz, $H^{5'}$ of O-bpy]; 9.01 [dd, 1H, $^3J_H{}^6{}_H{}^5$ = 5.4 Hz, $^4J_H{}^6{}_H{}^4$ = 1.2 Hz, $^3J_{PtH}{}^6$ = 20.5 Hz, H^6 of O-bpy]; 9.97 [d, 1H, $^3J_H{}^3{}_H{}^4$ = 8.3, H^3 of O-bpy]; $\delta(^{13}C\{H\})$ = -18.9 [s, 1C, $^1J_{PtC}$ = 677 Hz, Pt-Me]; 124.4 [s, 1C, $^2J_{PtC}{}^{3'}$ = 70.2 Hz, $C^{3'}$ of O-bpy]; 127.1 [s, 1C, $^3J_{PtC}{}^3$ = 20.5 Hz, C^3 of O-bpy]; 151.3 [s, 1C, $^2J_{PtC}{}^6$ = 21.3 Hz, C^6 of O-bpy]; 152.3 [broad signal, 1C, C of isocyanide]; 157.9 [s, 1C, $^2J_{PtC}{}^{1'}$ = 55.1 Hz, $C^{1'}$ of O-bpy]; 159.5 [s, 1C, $^1J_{PtC}{}^{2'}$ = 935 Hz, $C^{2'}$ of O-bpy]; $\delta(^{195}Pt)$ = -3903.8 [broad s, 1Pt].

[Pt(O-bpy)(Me)(CN-^{t}Bu)], 3a. To a solution of **A** (200 mg, 0.451 mmol) in CH_2Cl_2 (20 mL), 1 equivalent of CN-^{t}butyl (51 μL, 0.451 mmol, *tert*-butyl isocyanide) was added. The reaction mixture was stirred for 3 h at room temperature and then the solution was concentered to small volume (~ 3 mL) under reduced pressure and *n*-pentane (10 mL) was added to give **3a** as a yellow, which was filtered and washed with *n*-pentane (3 × 3 mL) and dried. Yield: 180 mg, 86%; m.p. = 162°C. Elem. Anal. Calcd. for $C_{16}H_{19}N_3OPt$ (464.42) C, 41.38; H, 4.12; N, 9.05. Found: C, 41.51; H, 4.19; N, 9.12. IR (KBr, cm^{-1}): 2172 (s, $\upsilon_{C\equiv N}$). NMR data in $CDCl_3$: $\delta(^1H)$ = 0.97 [s, 3H, $^2J_{PtH}$ = 84.2 Hz, Pt-Me]; 1.61 [s, 9H, CH_3 groups of tert-butyl]; 7.13 [dd, 1H, $^3J_H{}^{4'}{}_H{}^{3'}$ = 7.5 Hz, $^3J_H{}^{4'}{}_H{}^{5'}$ = 6.3 Hz, $H^{4'}$ of O-bpy]; 7.28 [ddd, 1H, $^3J_H{}^5{}_H{}^4$ = 7.8 Hz, $^3J_H{}^5{}_H{}^6$ = 5.4 Hz, $^4J_H{}^5{}_H{}^3$ = 1.2 Hz, H^5 of O-bpy]; 7.73 [dd, 1H, $^3J_H{}^{3'}{}_H{}^{4'}$ = 7.5 Hz, $^4J_H{}^{3'}{}_H{}^{5'}$ = 1.0 Hz, $^3J_{PtH}{}^{3'}$ = 56.0 Hz, $H^{3'}$ of O-bpy]; 8.0 [ddd, 1H, $^3J_H{}^4{}_H{}^3$ = 8.3 Hz, $^3J_H{}^4{}_H{}^5$ = 7.8 Hz, $^4J_H{}^4{}_H{}^6$ = 1.0 Hz, H^4 of O-bpy]; 8.04 [dd, 1H, $^3J_H{}^{5'}{}_H{}^{4'}$ = 6.3 Hz, $^4J_H{}^{5'}{}_H{}^{3'}$ = 1.0 Hz, $H^{5'}$ of O-bpy]; 8.79 [dd, 1H, $^3J_H{}^6{}_H{}^5$ = 5.4 Hz, $^4J_H{}^6{}_H{}^4$ = 1.0 Hz, $^3J_{PtH}{}^6$ = 20.2 Hz, H^6 of O-bpy]; 9.91 [d, 1H, $^3J_H{}^3{}_H{}^4$ = 8.3, H^3 of O-bpy]; $\delta(^{13}C\{H\})$ = -19.6 [s, 1C, $^1J_{PtC}$ = 685 Hz, Pt-Me]; 30.6 [s, 3C, CH_3 groups of tert-butyl]; 125.8 [s, 1C, $^3J_{PtC}{}^5$ = 13.2 Hz, C^5 of O-bpy]; 126.9 [s, 1C, $^3J_{PtC}{}^3$ = 19.9, C^3 of O-bpy]; 130.5 [s, 1C, $^2J_{PtC}{}^{3'}$ = 65.8 Hz, $C^{3'}$ of O-bpy], 138.4 [s, 1C, $C^{5'}$ of O-bpy]; 143.0 [broad signal, 1C, C of isocyanide]; 150.8 [s, 1C, $^2J_{PtC}{}^6$ =

20.5 Hz, C^6 of O-bpy]; 155.4 [s, 1C, $^2J_{PtC}{}^2$ = 31.4 Hz, C^2 of O-bpy]; 158.0 [s, 1C, $^2J_{PtC}{}^{1'}$ = 55.5 Hz, $C^{1'}$ of O-bpy]; 159.0 [s, 1C, $^1J_{PtC}{}^{2'}$ = 941 Hz, $C^{2'}$ of O-bpy]; δ(^{195}Pt) = -3956.7 [broad s, 1Pt].

***trans*-[Pt(O-bpy)(Me)$_2$I(CN-Bz)], 1b.** An excess amount of MeI (200 µL) was added to a solution of **1a** (100 mg, 0.201 mmol) in CH_2Cl_2 (20 mL) at room temperature. The reaction mixture was stirred for 5 h and then the solvent was evaporated under reduced pressure. The pale yellow residue was washed with *n*-pentane (3 × 3 mL) and dried under vacuum. Yield: 129 mg, 83%; m.p. = 168°C. Elem. Anal. Calcd. for $C_{20}H_{20}IN_3OPt$ (640.37) C, 37.51; H, 3.15; N, 6.56. Found: C, 37.38; H, 3.11; N, 6.61. IR (KBr, cm^{-1}): 2239 (s, $\upsilon_{C\equiv N}$). NMR data in $CDCl_3$: δ(^{1}H) = 0.98 [s, 3H, $^2J_{PtH}$ = 69.0 Hz, Pt-Me (Me *trans* to I)]; 1.57 [s, 3H, $^2J_{PtH}$ = 67.7 Hz, Pt-Me (Me *trans* to N)]; 5.15 [s, 2H, $^4J_{PtH}$ = 8.5 Hz, CH_2 of benzyl]; 7.13-7.54 [overlapping benzyl protons and H^5, H^4, $H^{4'}$ of O-bpy]; 7.57 [d, 1H, $^3J_H{}^{3'}{}_H{}^{4'}$ = 7.7 Hz, $^3J_{PtH}{}^{3'}$ = 41.1 Hz, $H^{3'}$ of O-bpy]; 8.08 [d, 1H, $^3J_H{}^{5'}{}_H{}^{4'}$ = 6.0 Hz, $H^{5'}$ of O-bpy]; 8.83 [d, 1H, $^3J_H{}^6{}_H{}^5$ = 5.0 Hz, $^3J_{PtH}{}^6$ = 10.2 Hz, H^6 of O-bpy]; 10.05 [d, 1H, $^3J_H{}^3{}_H{}^4$ = 8.0, H^3 of O-bpy]; δ(^{13}C{H}) = -7.3 [s, 1C, $^1J_{PtC}$ = 567 Hz, Pt-Me (Me *trans* to N)]; 3.8 [s, 1C, $^1J_{PtC}$ = 551 Hz, Pt-Me (Me *trans* to I)]; 48.6 [s, 1C, CH_2 of benzyl]; 127.1 [s, 2C, C^3 of benzyl]; 129.7 [s, 2C, C^2 of benzyl]; 148.7 [s, 1C, $^1J_{PtC}{}^{2'}$ = 788 Hz, $C^{2'}$ of O-bpy]; 155.6 [s, 1C, $^2J_{PtC}{}^{1'}$ = 37.3 Hz, $C^{1'}$ of O-bpy]; δ(^{195}Pt) = -3455.5 [broad s, 1Pt].

***trans*-[Pt(O-bpy)(Me)$_2$I(CN-2Np)], 2b.** An excess amount of MeI (200 µL) was added to a solution of **2a** (100 mg, 0.187 mmol) in CH_2Cl_2 (20 mL) at room temperature. The reaction mixture was stirred for 12 h and then the solvent was evaporated under reduced pressure. The pale brown residue was washed with *n*-pentane (3 × 3 mL) and dried under vacuum. Yield: 113 mg, 89%; m.p. = 231°C. Elem. Anal. Calcd. for $C_{23}H_{20}IN_3OPt$ (676.41) C, 40.84; H, 2.98; N, 6.21. Found: C, 40.76; H, 3.04; N, 6.29. IR (KBr, cm^{-1}): 2204 (s, $\upsilon_{C\equiv N}$). NMR data in $CDCl_3$: δ(^{1}H) = 1.13 [s, 3H, $^2J_{PtH}$ = 68.9 Hz, Pt-Me (Me *trans* to I)]; 1.69 [s, 3H, $^2J_{PtH}$ = 67.6 Hz, Pt-Me (Me *trans* to N)]; 7.55-8.07 [overlapping 2-naphtyl protons and the other protons of O-bpy]; 8.10 [d, 1H, $^3J_H{}^{5'}{}_H{}^{4'}$ = 6.2 Hz, $H^{5'}$ of O-bpy]; 9.10 [d, 1H, $^3J_H{}^6{}_H{}^5$ = 5.3 Hz, $^3J_{PtH}{}^6$ = 13.9 Hz, H^6 of O-bpy]; 10.07 [d, 1H, $^3J_H{}^3{}_H{}^4$ = 8.3, H^3 of O-bpy]; δ(^{13}C{H}) = -7.0 [s, 1C, $^1J_{PtC}$ = 567 Hz, Pt-Me (Me *trans* to N)]; 3.8 [s, 1C, $^1J_{PtC}$ = 550 Hz, Pt-Me (Me *trans* to I)]; 124.9 [s, 1C, $^2J_{PtC}{}^{3'}$ = 55.4 Hz, $C^{3'}$ of O-bpy]: 148.6 [s, 1C, $^1J_{PtC}{}^{2'}$ = 786 Hz, $C^{2'}$ of O-bpy]; 155.7 [s, 1C, $^2J_{PtC}{}^{1'}$ = 36.5 Hz, $C^{1'}$ of O-bpy]; δ(^{195}Pt) = -3453.6 [broad s, 1Pt].

***trans*-[Pt(O-bpy)(Me)$_2$I(CN-^{t}Bu)], 3b.** An excess amount of MeI (200 µL) was added to a solution of **3a** (100 mg, 0.215 mmol) in CH_2Cl_2 (20 mL) at room temperature. The reaction mixture was stirred for 3 h and then the solvent was evaporated under reduced pressure. The pale yellow residue was washed with *n*-pentane (3 × 3 mL) and dried under vacuum. Yield: 96 mg, 74%; m.p. = 173°C. Elem. Anal. Calcd. for $C_{17}H_{22}IN_3OPt$ (606.36) C, 33.67; H, 3.66; N, 6.93. Found: C, 33.81; H, 3.58; N, 6.82. IR (KBr, cm^{-1}): 2217 (s, $\upsilon_{C\equiv N}$). NMR data in $CDCl_3$: $\delta(^1H)$ = 0.95 [s, 3H, $^2J_{PtH}$ = 69.0 Hz, Pt-Me (Me *trans* to I)]; 1.53 [s, 3H, $^2J_{PtH}$ = 67.7 Hz, Pt-Me (Me *trans* to N)]; 1.70 [s, 9H, CH_3 groups of tert-butyl]; 7.16 [dd, 1H, $^3J_H{}^{4'}{}_H{}^{3'}$ = 6.6 Hz, $^3J_H{}^{4'}{}_H{}^{5'}$ = 6.6 Hz, $H^{4'}$ of O-bpy]; 7.38 [dd, 1H, $^3J_H{}^5{}_H{}^4$ = 7.1 Hz, $^3J_H{}^5{}_H{}^6$ = 5.6 Hz, H^5 of O-bpy]; 7.57 [d, 1H, $^3J_H{}^{3'}{}_H{}^{4'}$ = 7.7 Hz, $^3J_{PtH}{}^{3'}$ = 41.0 Hz, $H^{3'}$ of O-bpy]; 8.0 [dd, 1H, $^3J_H{}^4{}_H{}^3$ = 7.6 Hz, $^3J_H{}^4{}_H{}^5$ = 7.6 Hz, H^4 of O-bpy]; 8.07 [d, 1H, $^3J_H{}^{5'}{}_H{}^{4'}$ = 6.0 Hz, $H^{5'}$ of O-bpy]; 8.90 [dd, 1H, $^3J_H{}^6{}_H{}^5$ = 5.6 Hz, , $^4J_H{}^6{}_H{}^4$ = 1.3 Hz, $^3J_{PtH}{}^6$ = 12.6 Hz, H^6 of O-bpy]; 10.06 [d, 1H, $^3J_H{}^3{}_H{}^4$ = 8.4, H^3 of O-bpy]; $\delta(^{13}C\{H\})$ = -7.4 [s, 1C, $^1J_{PtC}$ = 570 Hz, Pt-Me (Me *trans* to N)]; 3.6 [s, 1C, $^1J_{PtC}$ = 555 Hz, Pt-Me (Me *trans* to I)]; 30.45 [s, 3C, CH_3 groups of tert-butyl]; 148.7 [s, 1C, $^1J_{PtC}{}^{2'}$ = 790 Hz, $C^{2'}$ of O-bpy]; 155.8 [s, 1C, $^2J_{PtC}{}^{1'}$ = 37.1 Hz, $C^{1'}$ of O-bpy]; $\delta(^{195}Pt)$ = -3444.3 [broad s, 1Pt].

Kinetic measurements

The kinetic rate constants were determined using UV-vis spectroscopy by monitoring the change in absorbance. A linear relationship between absorbance, *Abs*, and concentration, C, confirmed the validity of the Beer-Lambert law (*Abs* = εbC with b = path length = 1 cm) for all the complexes. All kinetic measurements were monitored under pseudo first-order conditions with MeI concentrations 5340-8900 times the concentration of the Pt(II) complexes. At least five different concentrations within this range were used. The concentration of Pt(II) complexes were 1.5 × 10^{-4} M. The activation parameters $\Delta H^{\neq}$ and $\Delta S^{\neq}$ for the reaction in CH_2Cl_2 were obtained from kinetic experiments performed at five temperatures between 10 and 35 °C. Pseudo first-order rate constants, k_{obs}, were calculated by fitting of the kinetic data to the first-order equation $Abs_t = Abs_\infty(Abs_0-Abs_\infty)\exp(-k_{obs}t)$. The experimentally determined pseudo first-order rate constants were converted to second-order rate constants, k_2, by determining the slope of the linear plots of k_{obs} against the concentration of the MeI at corresponding temperature according to equation $k_{obs}=k_2$[MeI]. The activation parameters were determined from the Eyring equation $\ln(k_2/T) = \ln(k_B/h) - \Delta H^{\neq}/RT + \Delta S^{\neq}/R$ with $\Delta H^{\neq}$ = activation enthalpy, $\Delta S^{\neq}$= activation entropy,

k_2= rate constant, k_B= Boltzmann's constant, T= temperature, h= Planck's constant, and R = universal gas constant.

Computational details

The geometries of complexes were fully optimized by employing the density functional theory without imposing any symmetry constraints. Density functional calculations were performed with the program suite Gaussian03[44] using the B3LYPlevel of theory[45-47]. The effective core potential of Hay and Wadt basis set (LANL2DZ) basis set was chosen to describe Pt and I atoms.[48, 49] The 6-31G(d) basis set was applied for the other atoms.

X-ray structure determinations

Single crystals of **1a** and **1b** were suitable for X-ray diffraction analysis. X-ray intensity data were collected using the full sphere routine by φ and ω scans strategy on the Agilent *SuperNova* dual wavelength EoS S2 diffractometer with mirror monochromated Mo *Kα* radiation (λ = 0.71073 Å). The crystal was cooled to 150 K using an Oxford Diffraction Cryojet low-temperature attachment. The data reduction, including an empirical absorption correction using spherical harmonics, implemented in *SCALE3 ABSPACK* scaling algorithm,[50] was performed using the *CrysAlisPro* software package.[51] The crystal structure was solved by direct methods using the online version of *AutoChem 2.0* in conjunction with *OLEX2* suite of programs implemented in the *CrysAlis* software.[52, 53] The non-hydrogen atoms were refined anisotropically. All of the hydrogen atoms were positioned geometrically in idealized positions and refined with the riding model approximation, with U_{iso}(H) = 1.2 or 1.5 U_{eq}(C). For the molecular graphics the program SHELXTL was used.[54] All geometric calculations were carried out using the *PLATON* software.[55] The iodide ligand in 1b is disordered over two position with a refined site occupancy ratio of 0.9712(8)/0.0288(8). Crystallographic data for the structural analysis has been deposited with the Cambridge Crystallographic Data Centre, No. CCDC-1577845 (**1a**) and CCDC-1577846 (**1b**).

Acknowledgments

This work was supported by the Institute for Advanced Studies in Basic Sciences (IASBS) Research Council and the Iran National Science Foundation (Grant no. 95834232). RK

is thankful to Sharif University of Technology research Council for the research facility (Grant No. QB960401). RK also thanks Prof. Paul R. Raithby and Bath University for their support. PRR is grateful to the Engineering and Physical Sciences Research Council (EPSRC) for continued funding (EP/K004956/1). Thanks are also due to Mr. A. Biglari, the operator of Bruker NMR instrument at IASBS, for recording the NMR spectra.

Supporting Information

Additional Supporting Information may be found online in the supporting information tab for this article.

References

[1] V. Sicilia, M. Baya, P. Borja, A. Martín, *Inorg. Chem.* **2015**, *54*, 7316.

[2] L. M. Rendina, R. J. Puddephatt, *Chem. Rev.* **1997**, *97*, 1735.

[3] S. M. Nabavizadeh, S. J. Hoseini, B. Z. Momeni, N. Shahabadi, M. Rashidi, A. H. Pakiari, K. Eskandari, *Dalton Trans.* **2008**, 2414.

[4] S. M. Nabavizadeh, E. S. Tabei, F. Niroomand Hosseini, N. Keshavarz, S. Jamali, M. Rashidi, *New J. Chem.* **2010**, *34*, 495.

[5] S. M. Nabavizadeh, H. R. Shahsavari, H. Sepehrpour, F. Niroomand Hosseini, S. Jamali, M. Rashidi, *Dalton Trans.* **2010**, *39*, 7800.

[6] M. Rashidi, M. Nabavizadeh, R. Hakimelahi, S. Jamali, *J. Chem. Soc., Dalton Trans.* **2001**, 3430.

[7] C. M. Anderson, R. J. Puddephatt, G. Ferguson, A. J. Lough, *J. Chem. Soc., Chem. Commun.* **1989**, 1297.

[8] C. M. Anderson, M. Crespo, M. C. Jennings, A. J. Lough, G. Ferguson, R. J. Puddephatt, *Organometallics* **1991**, *10*, 2672.

[9] R. H. Crabtree, The Organometallic Chemistry of the Transition Metals, in: The Organometallic Chemistry of the Transition Metals, John Wiley & Sons, Inc., **2014**.

[10] J. F. Hartwig, Organotransition Metal Chemistry: From Bonding to Catalysis, University Science Books, 2010.

[11] A. J. Canty, *Dalton Trans.* **2009**, 10409.

[12] W. B. Cross, E. G. Hope, Y.-H. Lin, S. A. Macgregor, K. Singh, G. A. Solan, N. Yahya, *Chem. Commun.* **2013**, *49*, 1918.

[13] Y. Boutadla, D. L. Davies, S. A. Macgregor, A. I. Poblador-Bahamonde, *Dalton Trans.* **2009**, 5820.

[14] D. L. Davies, S. M. Donald, O. Al-Duaij, S. A. Macgregor, M. Pölleth, *J. Am. Chem. Soc.* **2006**, *128*, 4210.

[15] D. L. Davies, S. M. Donald, S. A. Macgregor, *J. Am. Chem. Soc.* **2005**, *127*, 13754.

[16] S. Moncho, G. Ujaque, A. Lledós, P. Espinet, *Chem. Eur. J.* **2008**, *14*, 8986.

[17] M. Perez-Rodriguez, A. A. Braga, M. Garcia-Melchor, M. H. Pérez-Temprano, J. A. Casares, G. Ujaque, A. R. de Lera, R. Alvarez, F. Maseras, P. Espinet, *J. Am. Chem. Soc.* **2009**, *131*, 3650.

[18] G.-D. Roiban, E. Serrano, T. Soler, G. Aullón, I. Grosu, C. Cativiela, M. Martínez, E. P. Urriolabeitia, *Inorg. Chem.* **2011**, *50*, 8132.

[19] S. M. Nabavizadeh, H. Amini, F. Jame, S. Khosraviolya, H. R. Shahsavari, F. Niroomand Hosseini, M. Rashidi, *J. Organomet. Chem.* **2012**, *698*, 53.

[20] S. M. Nabavizadeh, M. Dadkhah Aseman, B. Ghaffari, M. Rashidi, F. Niroomand Hosseini, G. Azimi, *J. Organomet. Chem.* **2012**, *715*, 73.

[21] S. M. Nabavizadeh, H. Sepehrpour, R. Kia, A. L. Rheingold, *J. Organomet. Chem.* **2013**, *745–746*, 148.

[22] R. Babadi Aghakhanpour, S. M. Nabavizadeh, L. Mohammadi, S. Amini Jahromi, M. Rashidi, *J. Organomet. Chem.* **2015**, *781*, 47.

[23] P. Hamidizadeh, M. Rashidi, S. M. Nabavizadeh, M. Samaniyan, M. Dadkhah Aseman, A. M. Owczarzak, M. Kubicki, *J. Organomet. Chem.* **2015**, *791*, 258.

[24] M. Niazi, H. R. Shahsavari, *J. Organomet. Chem.* **2016**, *803*, 82.

[25] A. Nahaei, A. Rasekh, M. Rashidi, F. Niroomand Hosseini, S. M. Nabavizadeh, *J. Organomet. Chem.* **2016**, *815*, 35.

[26] S. M. Nabavizadeh, P. Hamidizadeh, F. A. Darani, F. Niroomand Hosseini, A. L. Rheingold, *Polyhedron* **2014**, *77*, 24.

[27] L. Maidich, A. Zucca, G. J. Clarkson, J. P. Rourke, *Organometallics* **2013**, *32*, 3371.

[28] A. Zucca, L. Maidich, L. Canu, G. L. Petretto, S. Stoccoro, M. A. Cinellu, G. J. Clarkson, J. P. Rourke, *Chem. Eur. J.* **2014**, *20*, 5501.

[29] S. Jamali, R. Czerwieniec, R. Kia, Z. Jamshidi, M. Zabel, *Dalton Trans.* **2011**, *40*, 9123.

[30] R. Babadi Aghakhanpour, M. Rashidi, F. Niroomand Hosseini, F. Raoof, S. M. Nabavizadeh, *RSC Adv.* **2015**, *5*, 66534.

[31] F. Raoof, M. Boostanizadeh, A. R. Esmaeilbeig, S. M. Nabavizadeh, R. Babadi Aghakhanpour, K. B. Ghiassi, M. M. Olmstead, A. L. Balch, *RSC Adv.* **2015**, *5*, 85111.

[32] S. J. Hoseini, S. M. Nabavizadeh, S. Jamali, M. Rashidi, *Eur. J. Inorg. Chem.* **2008**, *2008*, 5099.

[33] S. Jamali, S. M. Nabavizadeh, M. Rashidi, *Inorg. Chem.* **2005**, *44*, 8594.

[34] S. Jamali, S. M. Nabavizadeh, M. Rashidi, *Inorg. Chem.* **2008**, *47*, 5441.

[35] H. R. Shahsavari, R. Babadi Aghakhanpour, M. Babaghasabha, M. Golbon Haghighi, S. M. Nabavizadeh, B. Notash, *Eur. J. Inorg. Chem.* **2017**, *2017*, 2682.

[36] S. M. Nabavizadeh, H. Sepehrpour, H. R. Shahsavari, M. Rashidi, *New J. Chem.* **2012**, *36*, 1739.

[37] M. Crespo, M. Martínez, S. M. Nabavizadeh, M. Rashidi, *Coord. Chem. Rev.* **2014**, *279*, 115.

[38] M. E. Moustafa, P. D. Boyle, R. J. Puddephatt, *Organometallics* **2014**, *33*, 5402.

[39] H. R. Shahsavari, M. Fereidoonnezhad, M. Niazi, S. T. Mosavi, S. H. Kazemi, R. Kia, S. Shirkhan, S. Abdollahi Aghdam, P. R. Raithby, *Dalton Trans.* **2017**, *46*, 2013.

[40] H. R. Shahsavari, R. Babadi Aghakhanpour, M. Babaghassabha, M. Golbon Haghighi, S. M. Nabavizadeh, B. Notash, *New J. Chem.* **2017**, *41*, 3798.

[41] W. Schneider, K. Angermaier, A. Sladek, H. Schmidbaur, *Z. Naturforsch. B* **1996**, *51*, 790.

[42] M. Baya, Ú. Belío, J. Forniés, A. Martín, M. Perálvarez, V. Sicilia, *Inorg. Chim. Acta* **2015**, *424*, 136.

[43] B. S. Furniss, Vogel's textbook of practical organic chemistry, Pearson Education India, 1989.

[44] M. J. Frisch, N. Rega, G. A. Petersson, G. W. Trucks, H. Nakatsuji, M. Hada, M. Ehara, K. Toyota, R. Fukuda, J. Hasegawa, M. Ishida, J. C. Burant, T. Nakajima, Y. Honda, O. Kitao, H. B. Schlegel, H. Nakai, M. Klene, X. Li, J. E. Knox, H. P. Hratchian, J. B. Cross, J. M. Millam, V. Bakken, C. Adamo, J. Jaramillo, R. Gomperts, G. E. Scuseria, R. E. Stratmann, O. Yazyev, A. J. Austin, R. Cammi, C. Pomelli, S. S. Iyengar, J. W. Ochterski, P. Y. Ayala, K. Morokuma, G. A. Voth, P. Salvador, M. A. Robb, J. J. Dannenberg, V. G. Zakrzewski, S. Dapprich, A. D.

Daniels, J. Tomasi, M. C. Strain, O. Farkas, D. K. Malick, A. D. Rabuck, K. Raghavachari, J. B. Foresman, J. R. Cheeseman, J. V. Ortiz, Q. Cui, A. G. Baboul, V. Barone, S. Clifford, J. Cioslowski, B. B. Stefanov, G. Liu, A. Liashenko, P. Piskorz, I. Komaromi, J. A. Montgomery Jr, R. L. Martin, D. J. Fox, B. Mennucci, T. Keith, M. A. Al-Laham, C. Y. Peng, A. Nanayakkara, M. Challacombe, P. M. W. Gill, B. Johnson, W. Chen, T. Vreven, M. W. Wong, M. Cossi, C. Gonzalez, J. A. Pople, K. N. Kudin, G. Scalmani, *Gaussian 03, Revision C.02* **2004**.

[45] A. D. Becke, *J. Chem. Phys.* **1993**, *98*, 5648.

[46] B. Miehlich, A. Savin, H. Stoll, H. Preuss, *Chem. Phys. Lett.* **1989**, *157*, 200.

[47] C. Lee, W. Yang, R. G. Parr, *Phys. Rev. B* **1988**, *37*, 785.

[48] W. R. Wadt, P. J. Hay, *J. Chem. Phys.* **1985**, *82*, 284.

[49] L. E. Roy, P. J. Hay, R. L. Martin, *J. Chem. Theory Comput.* **2008**, *4*, 1029.

[50] R. C. Clark, J. S. Reid, *Acta Cryst.* **1995**, *A51*, 887.

[51] SuperNova Eos S2 System: Empirical absorption correction, **2011**, CrysAlis-Software package, Oxford Diffraction Ltd.

[52] O. V. Dolomanov, L. J. Bourhis, R. J. Gildea, J. A. K. Howard, H. Puschmann, *J. Appl. Cryst.* **2009**, *42*, 339.

[53] Agilent (**2012**): AutoChem 2.0, in conjunction with OLEX2. Agilent Technologies UK Ltd, Yarnton, Oxfordshire, England.

[54] A. Spek, *Acta Cryst.* **2009**, *D65*, 148.

[55] G. Sheldrick, *Acta Cryst.* **2008**, *A64*, 112.

Scheme and Figure Captions

Scheme 1. Synthetic route for the preparation of new complexes.

Scheme 2. S_N2 mechanism for the oxidative addition of MeI to Pt(II) center, resulting in the pure and stable *trans* product.

Scheme 3. Representative ligands with position labeling.

Figure 1. a) Perspective view of the structure of **1a** (left) and **1b** (right). Ellipsoids are drawn at the 40% probability level.

Figure 2. The crystal packing of **1a** viewed down the *a*-axis, showing *zigzag* connection of the neighboring molecules along the *b*-axis through C–H···O interactions.

Figure 3. The changes in the UV-vis spectrum of a) **1a**, b) **2a** and c) **3a** with MeI in CH_2Cl_2 at 25 °C (inset is the variation of absorbance at corresponding wavelength over time. Plots of the first order rate constants (k_{obs}/s^{-1}) versus MeI concentration, for the reactions of d) **1a**, e) **2a** and f) **3a** with MeI in CH_2Cl_2 under different temperature conditions.

Figure 4. Eyring plots for the reactions of **1a-3a** with MeI in CH_2Cl_2.

Figure 5. Optimized structures of **1a**, **TS** (transition state), **IMt** (intermediate for *trans*), **IMc** (intermediate for *cis*) and **1b**.

Figure 6. Energy profile for the oxidative addition of MeI to **1a** in CH_2Cl_2.

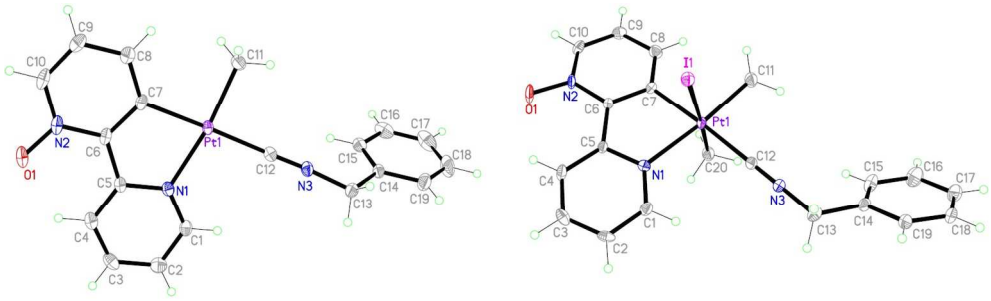

470x142mm (96 x 96 DPI)

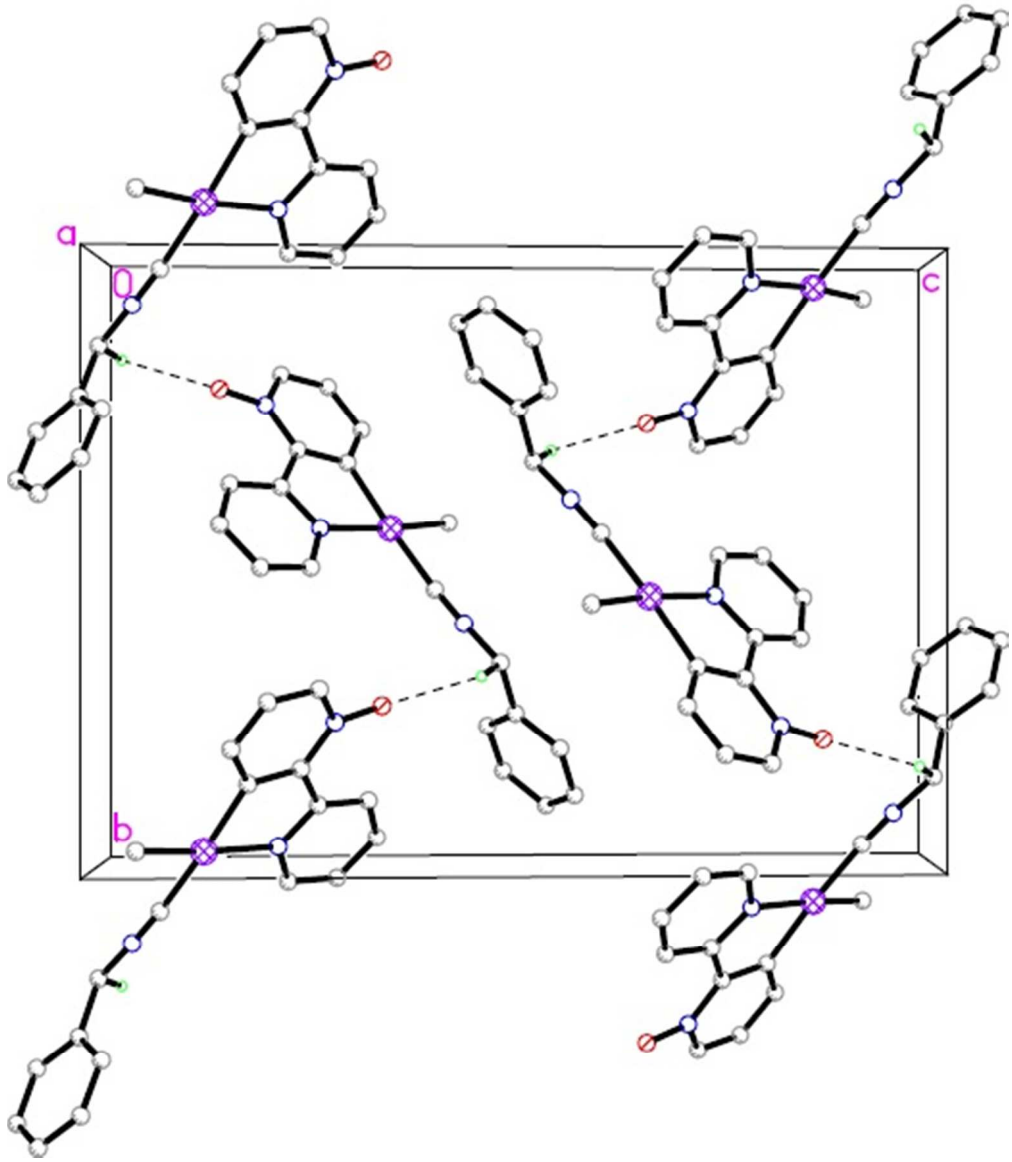

137x160mm (96 x 96 DPI)

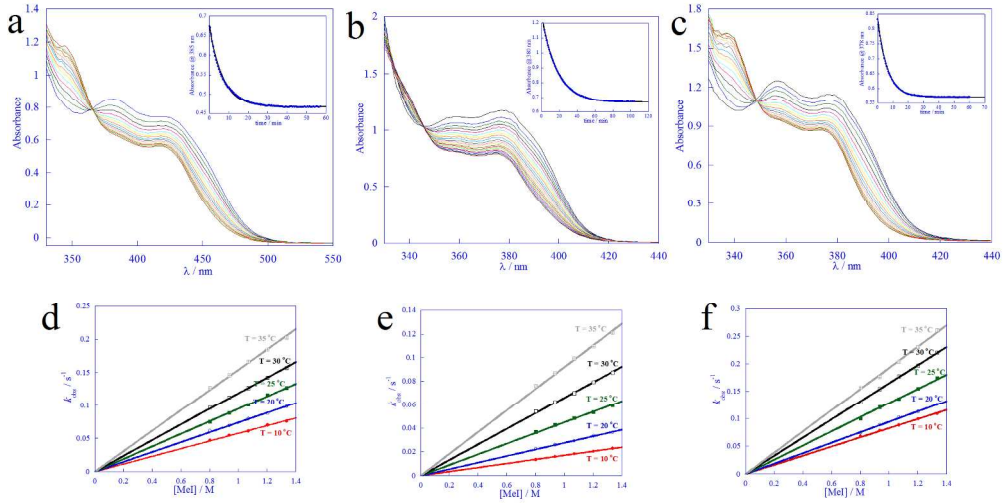

663x336mm (96 x 96 DPI)

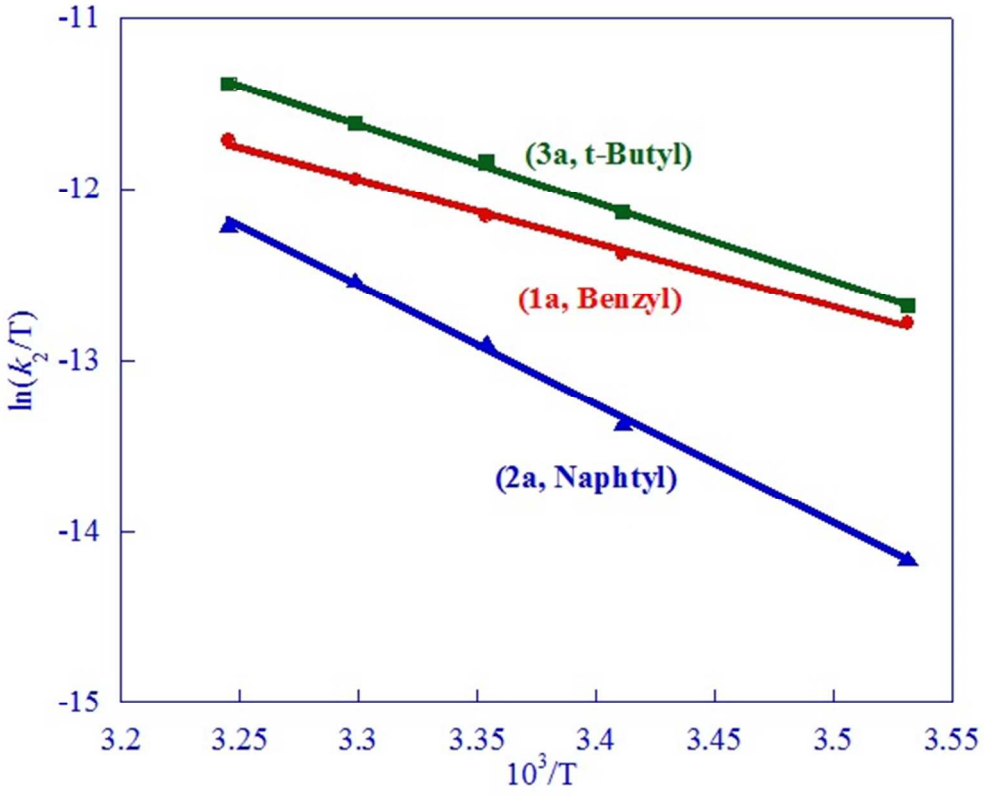

160x130mm (96 x 96 DPI)

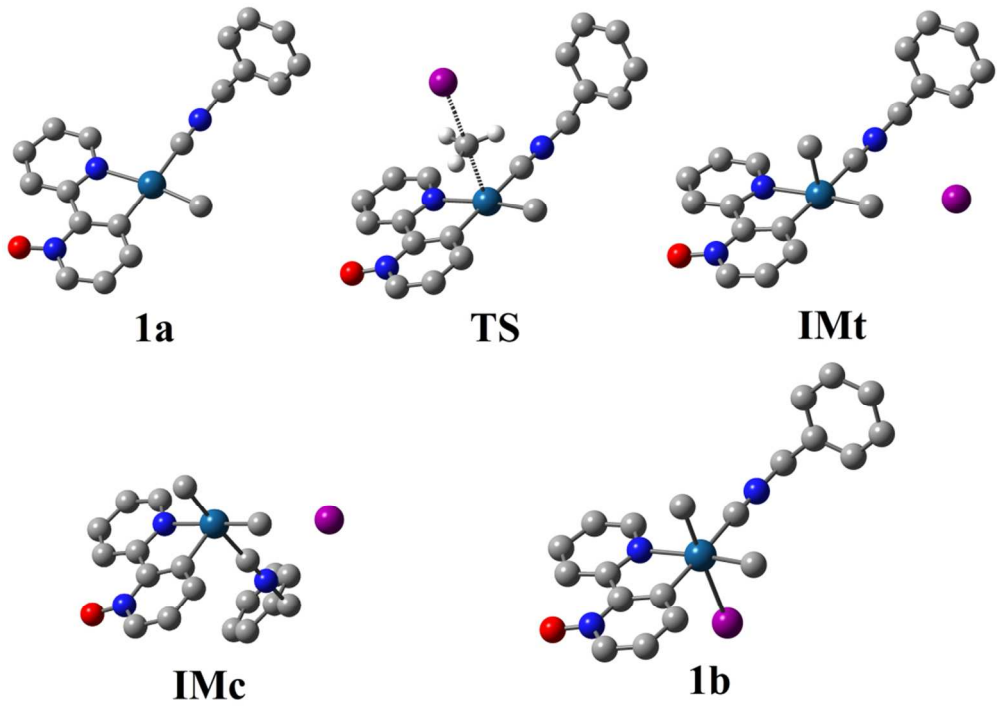

127x89mm (220 x 220 DPI)

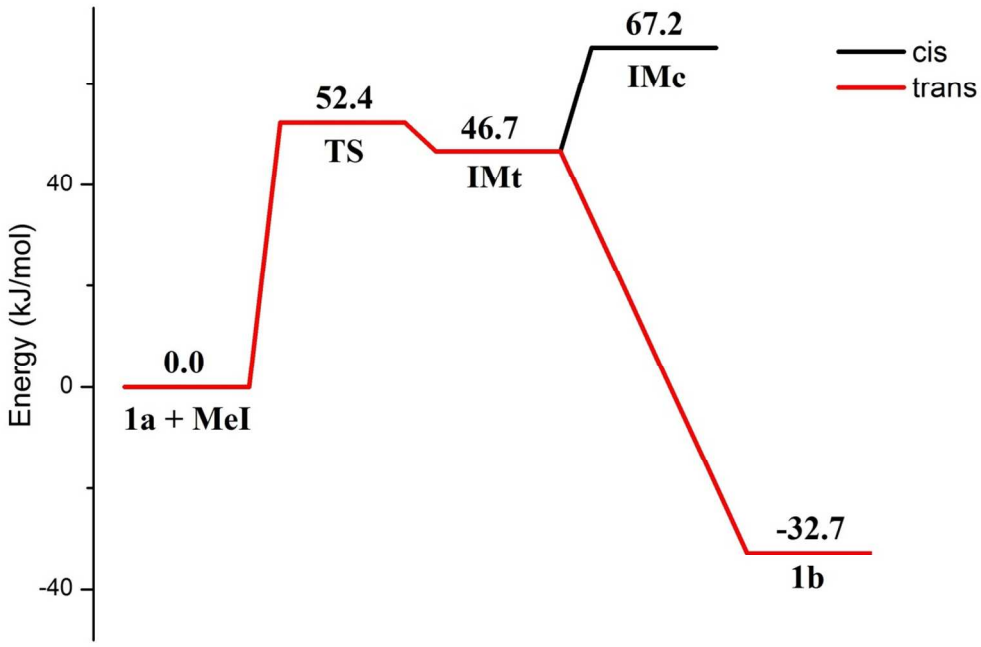

154x102mm (220 x 220 DPI)